

HINS_CH_SOL_06
 Fabrication Summary and Test Results

G. Davis, C. Hess, F. Lewis, D. Orris, M. Tartaglia, I. Terechkine, T. Wokas

I. Fabrication Summary

HINS_CH_SOL_06 is the second pre-production solenoid without correctors. The main goal of making and testing this solenoid was to check consistency in the performance. The solenoid was built from Main Coil (MC) serial number PPT1-02, and Bucking Coils (BC) BC15 and BC16.

The solenoid coils were wound from the same strand used in HINS_CH_SOL_05 [1]; namely 0.8mm NbTi strand (spool 6056-2, coated diameter 0.846 mm) was used to wind the main coil, and Oxford 0.6 mm NbTi strand (billet 8538-1B spool 1797A, coated diameter 0.634 mm) was used to wind the bucking coils. This is the same inventory of strand being used for final solenoid production, with critical parameters the same as in Tables 1 and 2 and Fig. 2 of [1]. Winding data of all the coils in the solenoid are almost identical to those in [1], but the distance between the main and the bucking coil is now 7.3 mm. This change has been made to eliminate spacers between the bucking coils and the flux return to simplify assembly. This new solenoid geometry did not change the solenoid quench point, although we also hoped to improve training by placing the winding of the bucking coil in slightly weaker magnetic field of the main coil. The as-built features of the solenoid are shown in Fig. 1 below.

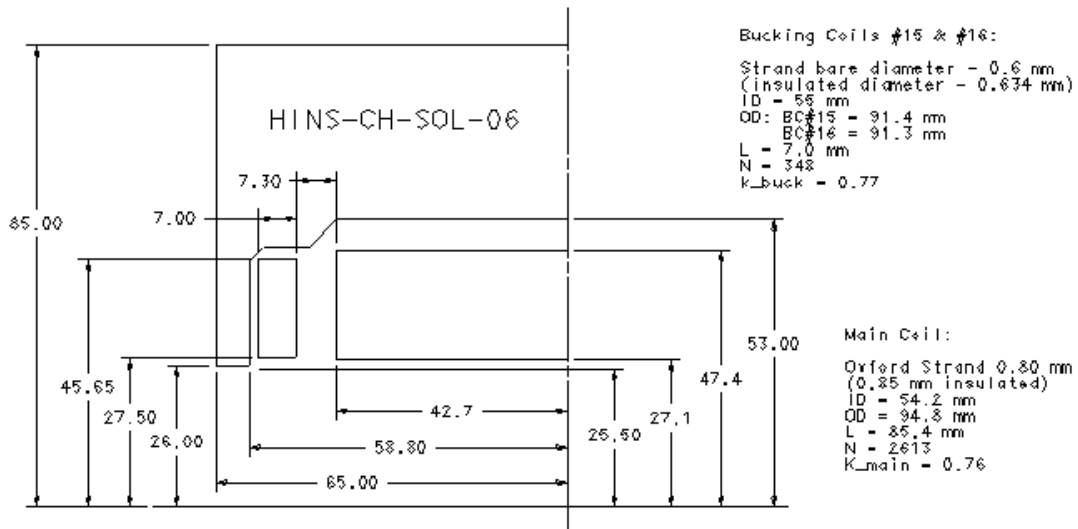


Fig. 1. HINS_CH-SOL-06 type 1 pre-production solenoid: as-built design features.

The limiting quench in the solenoid is expected to be in the Main Coil, at a current between 244 A and 250 A.

II. Test Overview

The cool down and cold power test took place on January 14, 2008. The helium temperature was maintained very consistently between 4.21 and 4.25 K, and about 850 liters of liquid helium were needed to complete the test. As in previous type 1 solenoid tests, we used a separate pair of leads for each of the three coils in the solenoid, so all connections between coils were made outside of the dewar. Fig. 2 shows the bus configuration for this test; the solenoid was oriented with BC16 above and BC15 below the main coil.

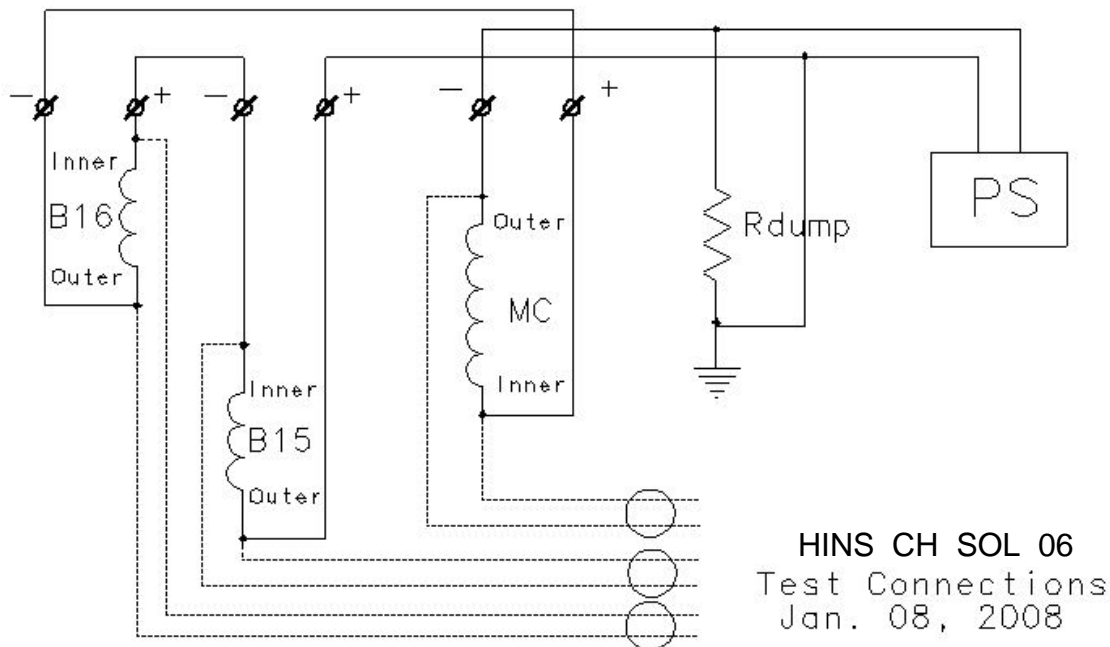


Fig. 2. Schematic of power connections (solid lines) and quench characterization voltage tap segments (dotted lines) across individual coils.

Warm magnetic measurements were made prior to cool down to confirm the proper relative field polarities of main and bucking coils. Quench training went fairly quickly. However, there were some power supply control problems, suspected of being due to ground loops with the non-isolated power supply drive inputs. In particular, the power supplies would not always reach the requested current, (e.g., instead of requested 260 A, it would deliver only 245 A). This was somewhat alleviated by changing the drive system transfer function slightly, but the power supply stability was not very good: the actual current drifted by several amperes during “constant current” magnet measurement profiles, and repeated stair-step current profiles did not reproduce accurately. Fortunately, the precision UNIX current readout provides a complete record of the behavior and accurate values for the analysis. Fig. 3 shows the UNIX current during the magnetic measurements, when four unexplained system trips also occurred.

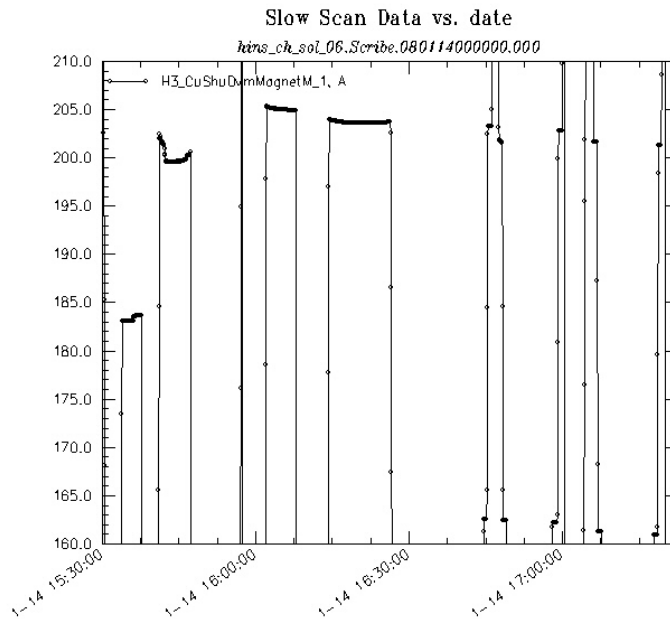


Fig. 3. Detail of UNIX current signal during magnetic measurement plateaus (for field shape scan) and stair-step profiles (for iron saturation study).

III. Quench Performance

Training was conducted with all three coils connected in series at a ramp rate of 1A/s, with a strictly enforced minimum of ten minutes between quenches. Figure 4 shows the training history: all quenches appear to have started in the Main Coil and the expected quench current was reached after 9 quenches.

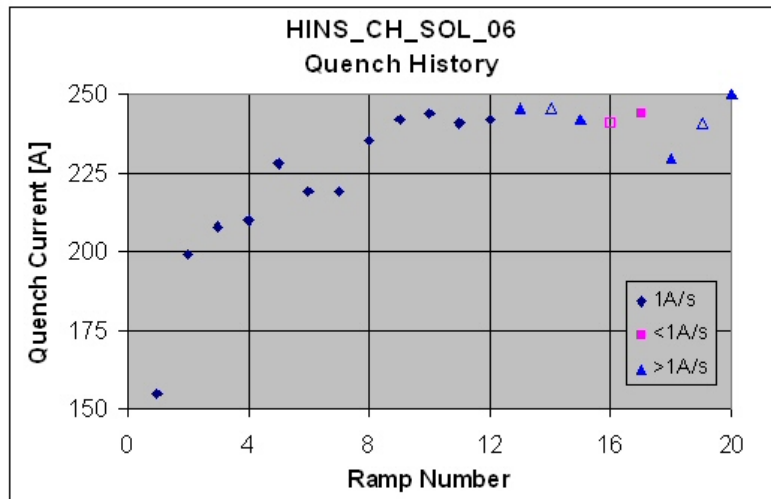


Fig. 4. Ramp history of hins_ch_sol_06; open symbols represent currents reached without quenching (because power supply delivered less than the requested current).

In almost all of the quenches both bucking coils showed one or more interesting voltage spikes followed by a damped ringing at a frequency of about 2 kHz; Fig. 5 shows an example of the symmetric but opposite polarity bucking coil ringing, which is suggestive of a mechanical shock to the yoke triggered by internal motion. These spikes often started at approximately the same time as the quench, but in some cases occurred well after the quench began. In many cases, one of the bucking coils appears to develop positive (resistive) voltage, and it is not always the same coil – so perhaps these quenches were developing in both main and bucking coils (triggered by mechanical shock?). At the highest currents (near the critical surface), there is clearly quench development in the BCs caused by large dI/dt , as the signals are initially inductive (negative), then change sign and rapidly increase – this had also been observed in early prototype solenoid tests. (We did not write much about the detailed quench development features since the test solenoids (pdst01-03); we simply discussed them as we were taking data, and tried to make sense of the signals).

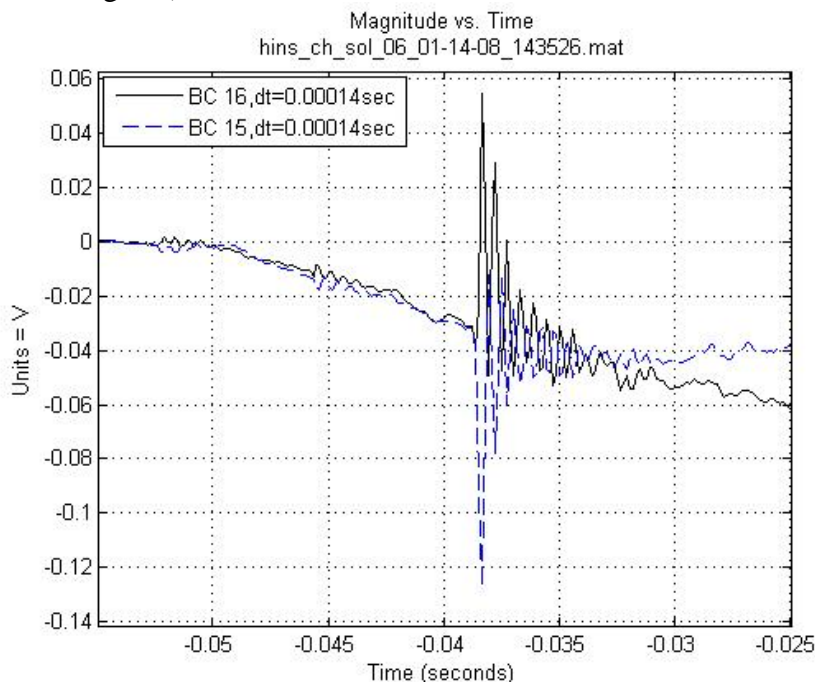


Fig. 5. Bucking Coil signals show ringing spike shortly after quench development starts in quench 13 (spike characteristics are typical of those seen in other quenches).

After training to a plateau, the sensitivity to ramp rate was explored. Fig. 6 shows the ramp rate dependence: the 1A/s plateau quench current varies by a couple of amperes, and there is not a strong variation until about 8 A/s. Interestingly, the best quench performance is obtained (consistently) with a ramp rate of 4 A/s; this correlates with similar behavior of HINS-CH-SOL-03d-1 [3]. A number of ramps to 245 A were made for magnetic measurements, without a quench, whereas lower ramp rates consistently quenched at or below this current level.

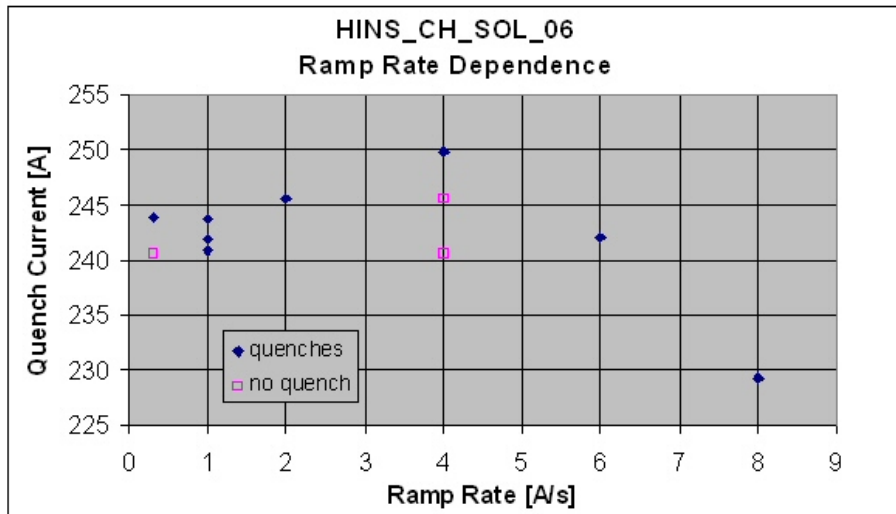


Fig. 6. Ramp rate dependence of quench current. The “no quench” points were again limited by the power supply.

IV. Magnetic Performance

Throughout this test, magnetic measurements were made using the “old” SENIS 3D Hall probe (ser. No 24-05) positioned “on-axis” in the G-10 probe support, as described and shown in Fig. 10 of [2]. The probe readout utilized the same Keithley 2700 multiplexing DMM as for previous tests with this probe, with recently improved shield grounding to reduce noise levels. Offset voltage levels were recorded as part of each measurement and subtracted in performing the analysis. The RMS noise levels were less than 5 Gauss for each of the three elements. A single measurement was taken for each position during z-scans, and 10 measurements were taken at each current during stair-step studies.

A 2-D model was constructed using the Vector Fields program OPERA, which incorporated the as-built (warm) geometry and coil winding parameters, both with and without a gap in the iron flux return yoke; the actual solenoid was built with a 0.5 ± 0.12 mm gap, which is expected to become 0.2 mm after cooling down. The model utilized the program default “soft iron” material B-H properties, isotropic with a permeability of 500, and calculations used the non-linear material analysis.

Measurements made at different current levels demonstrated that the predicted solenoid parameters are quite close to the observed ones. Fig. 7 compares the predicted and measured magnetic field along the axis of the solenoid at 200 A.

The solenoid transfer function shows some nonlinear behavior as a function of current that slightly affects its central field and, to a greater extent, its fringe field. Fig. 8 shows the model prediction of transfer function in the center of the solenoid, and Fig. 9 in the fringe region 150 mm from the solenoid center, for different currents. The solenoid is very symmetric, shows no hysteresis, and the model is in good agreement with the measurements.

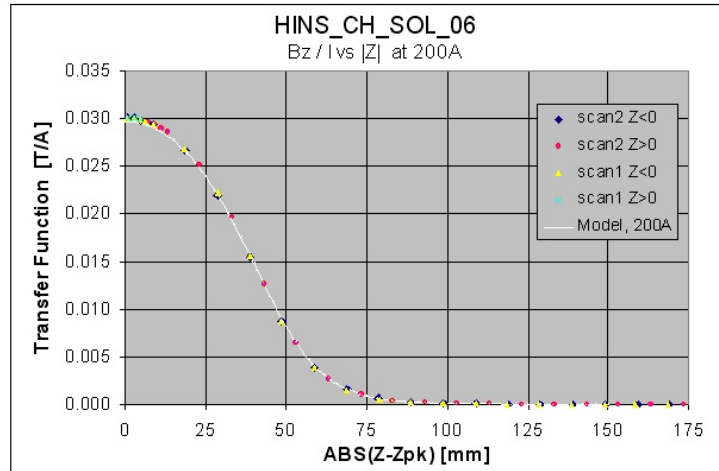


Fig. 7. Comparison of model and data axial field transfer function profiles at 200A: data peak is 1.2% higher than predicted.

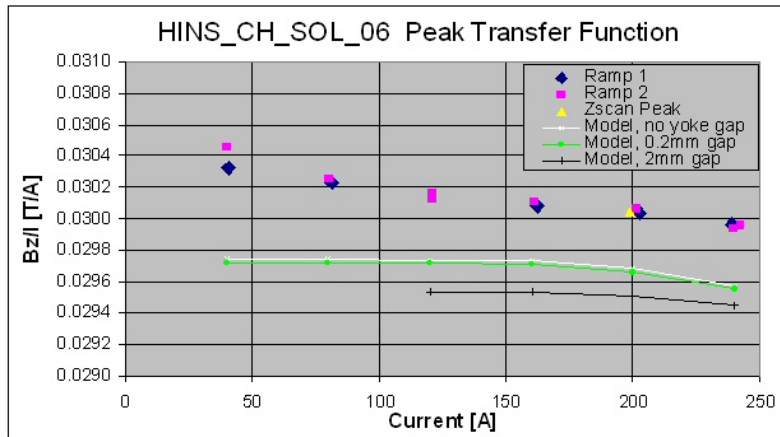


Fig. 8. Transfer function versus current at the solenoid center, with model predictions for a range of iron yoke gap widths.

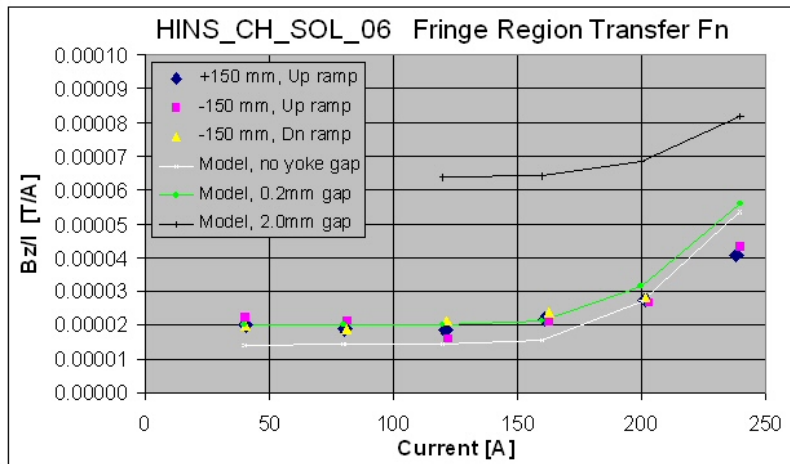


Fig. 9. Comparison of model and data, current dependence of axial field transfer function profiles at 150 mm from the solenoid center.

V. Conclusions

This test completes the series of R&D solenoid fabrication and testing for the CH section of HINS, with the second pre-production type 1 lens. The magnet trained rather quickly to the expected main coil quench current level, and showed weak ramp rate dependence of the quench current. The axial magnetic field on the solenoid axis matches the predicted behavior quite well, both at the center and in the fringe regions, in terms of absolute strength and dependence on current, due to iron saturation. This solenoid is therefore acceptable for use in the HINS CH beam line.

References

- [1] E. Barzi, G. Davis, C. Hess, F. Lewis, D. Orris, M. Tartaglia, I. Terechkine, D. Turrioni, T. Wokas, "HINS_CH_SOL_05", FNAL TD Note, TD-07-027, FNAL, 30 Oct 2007.
- [2] C. Hess, F. Lewis, D. Orris, M. Tartaglia, I. Terechkine, T. Wokas, "Focusing Solenoid HINS_CH_SOL_02 Fabrication Notes and Test Results", FNAL, TD-07-008, May 09, 2007.
- [3] G. Davis, C. Hess, F. Lewis, D. Orris, M. Tartaglia, I. Terechkine, T. Wokas, "HINS_CH_SOL_03d-1 Fabrication Notes and Test Results", FNAL TD Note, TD-08-002, FNAL, Jan. 30, 2008.